NANO LETTERS

pubs.acs.org/NanoLett

Stretchable Graphene: A Close Look at Fundamental Parameters through Biaxial Straining

Fei Ding,[*,†,§] **Hengxing Ji,**[*,†] **Yonghai Chen,**[§] **Andreas Herklotz,**[‡] **Kathrin Dörr,**[‡] **Yongfeng Mei,**[*,†,∥] **Armando Rastelli,**[†] **and Oliver G. Schmidt**[†]

[†]Institute for Integrative Nanosciences and [‡]Institute for Metallic Materials, IFW Dresden, Helmholtzstrasse 20, D-01069 Dresden, Germany and [§]Key Laboratory of Semiconductor Materials Science, Institute of Semiconductors, Chinese Academy of Sciences, Beijing 100083, China

ABSTRACT Tunable biaxial stresses, both tensile and compressive, are applied to a single layer graphene by utilizing piezoelectric actuators. The Grüneisen parameters for the phonons responsible for the D, G, 2D and 2D′ peaks are studied. The results show that the D peak is composed of two peaks, unambiguously revealing that the 2D peak frequency (ω_{2D}) is not exactly twice that of the D peak (ω_D). This finding is confirmed by varying the biaxial strain of the graphene, from which we observe that the shift of $\omega_{2D}/2$ and ω_D are different. The employed technique allows a detailed study of the interplay between the graphene geometrical structures and its electronic properties.

KEYWORDS Graphene, strain engineering, Grüneisen parameters, Raman spectroscopy, piezoelectric actuator

Graphene is attracting intense attention owing to its unique physical properties arising from the two-dimensional hexagonal lattice structure.[1-3] Various interesting phenomena have been observed in graphene, including the quantum Hall effect,[4,5] ultrahigh mobility,[6] superior thermal conductivity,[7,8] and high mechanical strength.[9] These unusual properties make graphene a promising material for building blocks in nanoelectronic devices.[1]

Much of the interest in graphene arises from the interplay between the geometrical structure and electronic properties. For example, substrate-induced sublattice symmetry breaking in epitaxially grown graphene can give rise to energy gaps in the electronic structures;[10] scanning tunneling microscopy (STM) studies show evidence for strain-induced spatial modulations in the local conductance of graphene on SiO_2;[11] and calculations predict that strain with triangular symmetry could induce strong gauge fields that effectively act as a uniform magnetic field exceeding 10 T.[12] However, most of these studies are based on simulations, or on graphene layers with fixed strain. Thus, new techniques allowing for strain on demand are important to intentionally tune and understand the interplay between geometry and electronic properties of graphene.

Uniaxial strain on graphene has been experimentally studied by bending graphene on a plastic substrate and using Raman spectroscopy to probe its phonon modes.[13-17] The Grüneisen parameters, which are crucial for correct theoretical treatment of phonon transport and thermal conductivity in graphene,[18,19] have been extracted from the experimental values, and the splitting of the G peak into two bands was observed.[14] However, uniaxial strain moves the relative positions of the Dirac cones and has a significant influence in the intervalley double-resonance processes (D and 2D peaks). Thus, biaxial strain, which avoids such perturbations and mimics the realistic experimental conditions where the graphene is supported by a planar substrate, would be more suited to study the strain effects on the double-resonance processes. In fact Metzger et al. studied graphene spontaneously adhered to the bottom of small aspect ratio depressions, resulting in a fixed biaxial strain of ~0.066%.[20] There is a significant discrepancy between their reported Grüneisen parameters, the calculated values by first principles, and that extrapolated from uniaxial data by Mohiuddin et al.[14]

In this letter, we report a method relying on a piezoelectric substrate to apply a tunable biaxial stress to graphene. By careful optimization of interfacial layers, the single layer graphene (SLG) is made visible on a $[Pb(Mg_{1/3}Nb_{2/3})O_3]_{0.72}$-$[PbTiO_3]_{0.28}$ (PMN-PT) substrate. With this electro-mechanical device we can apply biaxial compressive or tensile stress to graphene, allowing for smooth variations of strain. The Raman spectra measured at different strain values are fully reproducible over multiple compressing/stretching cycles without hysteresis. The Grüneisen parameters of graphene under biaxial strain are extracted from data. We also study the disorder-induced double resonance D peak and its overtone, the 2D peak. It is shown that ω_{2D} (the 2D mode frequency) is not exactly twice that of ω_D (the D mode frequency). This interesting finding is further confirmed by

---

[*] To whom correspondence should be addressed. E-mail: f.ding@ifw-dresden.de (F.D.), h.ji@ifw-dresden.de, (H.J.), y.mei@ifw-dresden.de (Y.M.).

[∥] Department of Materials Science, Fudan University, Shanghai, 200433, China.

Received for review: 04/30/2010
Published on Web: 08/09/2010

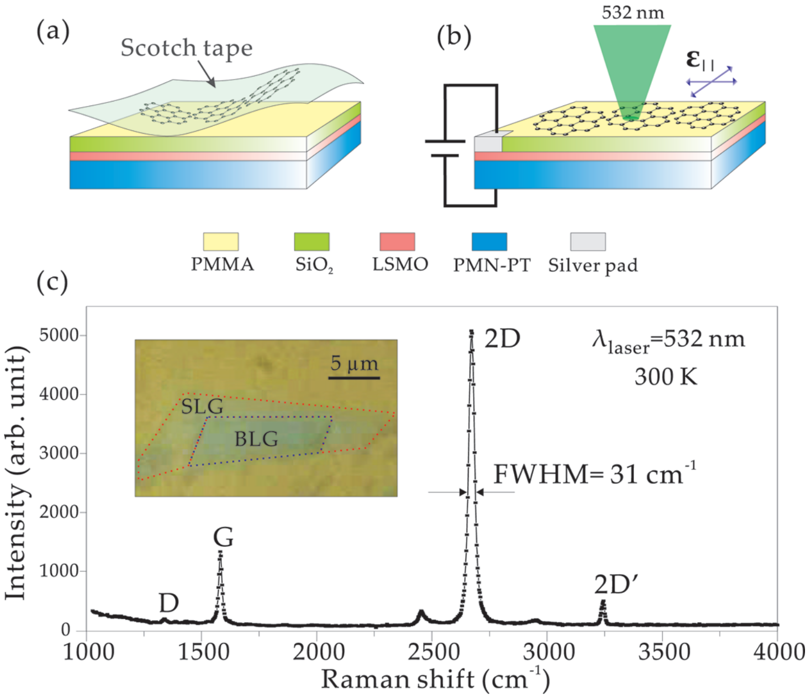

FIGURE 1. (a) Mechanical cleavage technique with a scotch tape is used to fabricate graphene which is then transferred, using a thin layer of PMMA as glue, onto a SiO_2/LSMO covered PMN-PT substrate. (b) Schematic drawing of the electro-mechanical device used to apply in-plane biaxial strain to the graphene. (c) Typical Raman spectrum (measured at 300 K) of SLG that is transferred onto a piezoelectric substrate. The inset shows an optical microscopy image of the SLG as well as of a BLG (bilayer graphene).

varying the temperature or changing the biaxial strain of the graphene, from which we see $\omega_{2D}/2$ and ω_D shift at different rates. This peculiar "$\omega_{2D}/2 \neq \omega_D$" phenomenon has been predicted for two-dimensional graphite,[21,22] and was observed in several studies of different types of sp^2 carbon materials.[21,23] However, recent studies of single layer graphene showed controversial results.[24−26] Our results indicate that the discrepancy between different reports may be due to the different intrinsic strain in the graphene samples.

The biaxial strain is provided by a 300 μm thick PMN-PT substrate overgrown with a thin (~40 nm) epitaxial layer of $La_{0.7}Sr_{0.3}MnO_3$ (LSMO) acting as top contact. The backside is coated with gold. A bias voltage V applied to the PMN-PT results in an out-of-plane electric field F which leads to an in-plane strain $\varepsilon_{||}$. After the deposition of a 1 μm thick SiO_2 layer, the substrate is spin-coated with a 60 nm thick PMMA (polymethyl methacrylate) layer. We fabricate the graphene samples from highly ordered pyrolytic graphite (HOPG) by mechanical cleavage[2] with the scotch tape technique. The tape is then placed onto the substrate followed by a baking process at 120 °C for 5 min (Figure 1a). The gluelike PMMA layer becomes solid and the graphene layers are transferred onto the piezoelectric actuator (Figure 1b). It is worth mentioning that the thickness of the interfacial SiO_2/PMMA layers has been carefully optimized to visualize the SLGs under an optical microscope.

The definitive identification of the SLGs is provided by Raman spectroscopy.[26] The measurements are performed at either room or low temperature (15 K) with a Helium-flow cryostat which uses a laser ($\lambda_{Laser} = 532$ nm) as excitation source. The laser power is kept low to avoid laser induced heating. A 100× objective with numerical aperture 0.7 is used to collect Raman signals, while a holographic notch filter cuts the Rayleigh scattered light. The peaks observed in the Raman spectra are fitted with Lorentzians to precisely determine the positions of each peak.

Figure 1c shows the typical Raman spectrum (measured at 300 K) of a SLG after transfer onto the piezoelectric substrate. The optimization of the interfacial SiO_2/PMMA layers ensures a good optical contrast (see inset of Figure 1c) as well as a sufficient Raman intensity for the study of graphene on a piezoelectric substrate. The characteristic Raman features are the so-called D, G, 2D and 2D′ peaks, which lie at 1339, 1581, 2671, and 3245 cm^{-1} respectively. The D peak is explained as originating from an intervalley double resonance (DR) which involves transitions near two inequivalent **K** points at neighboring corners of the hexagonal first Brillouin zone of graphene and requires a defect for its activation.[27,28] The G peak corresponds to the doubly degenerate E_{2g} phonon at the Brillouin zone center. The 2D peak is the second order of the D peak in which the momentum conservation is obtained by the scattering of two phonons with opposite wave vectors (**q** and **-q**), so that the 2D peak does not require the presence of defects for its activation. The 2D′ peak is the second order of the so-called D′ peak which originates from the intravalley DR process connecting two points belonging to the same cone around **K** (or **K′**). Here we observe the Raman fingerprint of SLG, a

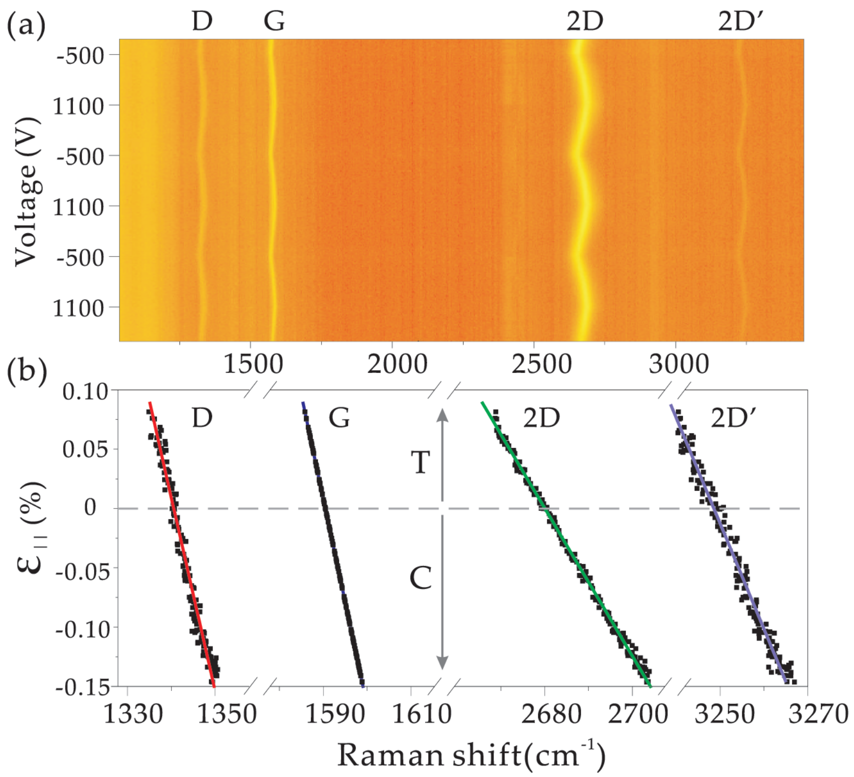

FIGURE 2. (a) Color-coded intensity map of the Raman peaks of one SLG sample as a function of the voltage applied to the PMN-PT actuator. The Raman spectra measured at different strain are fully reproducible over multiple compressing/stretching cycles without hysteresis. (b) D, G, and 2D peaks plotted as a function of the biaxial strain $\varepsilon_{||}$, the solid lines are linear fits. Both tensile strain (T) and compressive strain (C) are feasible with the piezoelectric actuator.

single sharp 2D peak with a fwhm (full width at half-maximum) of about 31 cm^{-1} and an intensity which is roughly 4 times of that of the G peak, agreeing well with previous literature.[26]

One of the advantages of the PMN-PT crystal is that it is capable of exerting either compressive or tensile stress at very low temperature. Figure 2a presents the color-coded intensity map of the Raman peaks of a SLG sample as a function of the voltage V applied to the PMN-PT actuator (measured at 15 K). V is swept several times between −550 and 1100 V with steps of 20 V to demonstrate the reversibility of the strain tuning technique. The maximum voltage is only limited by our power supply. Thinner PMN-PT substrates would allow us to achieve the same out-of-plane electric field F (therefore, the same in-plane strain $\varepsilon_{||}$) with much smaller voltages. For $V < 0$, the graphene experiences an in-plane tension (T) and the Raman peaks show roughly linear shifts to lower frequencies, as reported before.[13−15] In-plane compression (C) on the graphene is also feasible with this piezoelectric actuator, just by applying a positive voltage $V > 0$ to the substrate. From Figure 2a we do not see any hysteresis over multiple compressing/stretching cycles.

The Grüneisen parameters describe the strain sensitivity of the phonon frequencies and are thus an important fundamental set of parameters for graphene. There have been several attempts to measure the Grüneisen parameters under uniaxial strain[13−15,17] or hydrostatic strain.[29] As discussed before, the D and 2D peaks are zone-boundary phonons activated by intervalley double resonances, and the relative movement of the Dirac cones changes the phonon wave vector we are probing.[14] Therefore, it would be more suitable to measure the D mode Grüneisen parameter under biaxial strain, as shown below. The Grüneisen parameter γ is defined as

$$\gamma = -\frac{1}{2\omega^0}\frac{\partial\omega}{\partial\varepsilon_{||}} \tag{1}$$

where $\varepsilon_{||}$ is the biaxial strain of the graphene, and ω^0 and ω are the Raman frequencies at zero strain and under finite strain, respectively. To obtain the values of $\varepsilon_{||}$ in the graphene layer, we use the Grüneisen parameter of the G peak ($\gamma_G = 1.8$), which was obtained by the first-principles calculations by Mohiuddin et al.[14] and is a reasonable value for sp^2 carbon materials.[14,29−31] The maximum compressive strain at $V = 1100$ V is ∼−0.15%, in good agreement with our previous experiments on PMN-PT substrates.[32,33] After the strain calibration, we can plot the strain-dependent shifts of D, 2D, and 2D′ peaks in Figure 2b. All peaks show smooth and linear shifts with biaxial strain, indicating that neither slippage nor corrugation of the graphene occurs during the experiment.

Linear fits of all data (under either compressive or tensile strain) yield $\partial\omega_G/\partial\varepsilon_{||}$ ∼−57.3, $\partial\omega_D/\partial\varepsilon_{||}$ ∼−61.3, $\partial\omega_{2D}/\partial\varepsilon_{||}$ ∼−160.3, and $\partial\omega_{2D'}/\partial\varepsilon_{||}$ ∼−112.4 cm^{-1}/%. With eq 1, we

TABLE 1. Raman Peak Variation As a Function of Applied Biaxial Strain (Defined by $\partial\omega/\partial\varepsilon_{||}$, $cm^{-1}/\%$), Compared with the Values That Are Summarized in Reference 14[a]

	$\partial\omega/\partial\varepsilon_{\|\|}$ (Grüneisen parameters)			
Peak	this work	sp^2 carbon materials	extracted from uniaxial values	first-principles calculations
G	−57.3 (1.80)	−55∼−60 (1.72−1.9)	−63 (1.98)	−58 (1.8)
D	−61.3 (2.30)	N.A.	N.A.	N.A.
2D	−160.3 (2.98)	−154 (2.84)	−191 (3.55)	144 (2.7)
2D′	−112.4 (1.73)	−113 (1.74)	−104 (1.61)	N.A.

[a] The Grüneisen parameters extracted from the biaxial straining experiments are also given.

obtain the Grüneisen parameters $\gamma_D = 2.30$, $\gamma_{2D} = 2.98$, and $\gamma_{2D'} = 1.73$. Our results are in good agreement with values derived from first-principles calculations for graphene,[14] and experimental values for carbon materials under hydrostatic pressure(for example, carbon fibers and graphite[14]), suggesting that graphene has similar strain dependencies of the Raman frequencies with graphite.[29] There are some differences between our results and the values derived from uniaxial experiments,[13−15,17] which might be explained by the reasons stated above.

Even more important we see that the Grüneisen parameters are different for the D peak and its overtone 2D peak ($\gamma_D = 2.30$ and $\gamma_{2D} = 2.98$), the latter value agreeing well with previous reports (see Table 1). We observe this phenomenon also during the cooling of the sample from 300 to 15 K; see Figure 3a. It is clear that the G and 2D peaks shift toward higher frequencies with decreasing temperature, and the temperature coefficients[34,35] are ∼−0.025 and ∼−0.032 cm^{-1}/K, respectively. However we do not observe a significant shift in the D peak frequency with changes in temperature. This is surprising, considering that the 2D peak shows a large shift of nearly 9 cm^{-1}, so that the peak position of the D peak (ω_D) should shift by $\omega_{2D}/2 \sim 4.5$ cm^{-1}. Our observations are in line with the reports by Calizo et al. and Allen et al. who studied the temperature dependence behaviors of the 2D peak[34] and D peak,[35] respectively. Since thermal expansion constitutes an essential part of the temperature dependent Raman shift behavior, Figure 3a already indicates different strain sensitivities of the D and 2D peaks.

A closer look at Figure 2b is given in Figure 3b, where the half of ω_{2D} is plotted together with ω_D as a function of $\varepsilon_{||}$. Under tensile strain ($\varepsilon_{||} > 0$) ω_D is slightly larger than $\omega_{2D}/2$, which is in agreement with several prior Raman studies of different types of sp^2 carbon materials.[21,23,36] With increasing compressive strain both Raman peaks shift linearly to higher frequencies, with ω_D having a smaller slope (i.e., a smaller Grüneisen parameter) than $\omega_{2D}/2$. Similar results can be observed in the study of SiO_2-layer-capped-graphene by Ni et al.,[24] where the annealing temperature of the capping layer was changed, thus introduced compressive biaxial stress to the graphene. In addition to the blue shift of the Raman modes, one can observe the different shift rates for ω_D and $\omega_{2D}/2$ with annealing temperature.[24] In Figure 3b, when $\varepsilon_{||} \sim -0.025\%$ we find $\omega_D = \omega_{2D}/2$. However, the fwhm of the D peak does not show a monotonic change with external strain (see inset of Figure 3b). Although we have increased the data acquisition time for the D mode Raman signal and repeated the measurement for several cycles, the data show a rather discrete behavior with a butterfly like pattern (indicated by the red dashed lines). Corresponding to the strain where $\omega_D = \omega_{2D}/2$, the D peak fwhm shows a minimum value of ∼17 cm^{-1}.

In the following, we discuss a possible mechanism leading to the peculiar behavior of the D mode. It was proposed that the Raman D mode of two-dimensional graphite consists of two peaks, though their origin is still under discussion.[21,22] We follow the discussion by Cançado et al. and distinguish the two peaks by whether the first scattering of an electron is by a phonon or by a defect.[21] The D mode is associated with the intervalley DR scattering,[27,28] involving transitions near **K** and **K′** points. For one possibility, as depicted in the upper panel of Figure 3c, an electron with wavevector **k** near the **K** point is resonantly excited, by absorbing a photon of energy E_{Laser}, from the π band to the π^* band. The electron is then inelastically scattered by a phonon of wavevector q_1 to a point belonging to a circle around the **K′** point. The elastic backscattering is activated by a defect (or, by the graphene edge), and the electron goes back to the **k** state and recombines with a hole. The second possibility, as depicted in the lower panel of Figure 3c, consists of a reversed time sequence for the elastic and inelastic scattering, involving a phonon of wavevector q_2. These two mechanisms lead to Raman peaks with slightly different frequencies (ω_{D_1} and ω_{D_2}). Other mechanisms might be possible,[21] however they also lead to the D_1 and D_2 Raman peaks. The 2D peak involves two q_1 phonons, and thus its frequency equals $2 \times \omega_{D_1}$.

To support the above hypothesis, we analyze the line shape of the D and 2D peaks at a tensile strain $\varepsilon_{||} \sim 0.075\%$ in the left part of Figure 4. The horizontal scale for the 2D peak is on the upper axis of Figure 4 and is divided by two in order to superimpose D and 2D in the same figure. We have increased significantly the acquisition time to gain enough photon counts for the weak D peak, and we have repeated the measurement 10 times to ensure an accurate evaluation of the D peak line shape. The 2D peak shows a single Lorentzian shape with a fwhm of ∼32 cm^{-1} (with the contribution from phonon with wave-vector q_1), while the D peak shows a similar Lorentzian but with a small high-energy shoulder. Two Lorentzians with the same fwhm are used to fit the D peak.[21,22] It is interesting to note that one of the fitted peaks has the same frequency as $\omega_{2D}/2$ and the fitted fwhm is ∼16 cm^{-1} (half of the 2D peak fwhm). This peak involves a contribution from phonon q_1, and the other one from phonon q_2. However, in experiments a single Lorentzian is normally used to determine the D peak position, which is why the measured ω_D is slightly larger than $\omega_{2D}/2$ and the measured

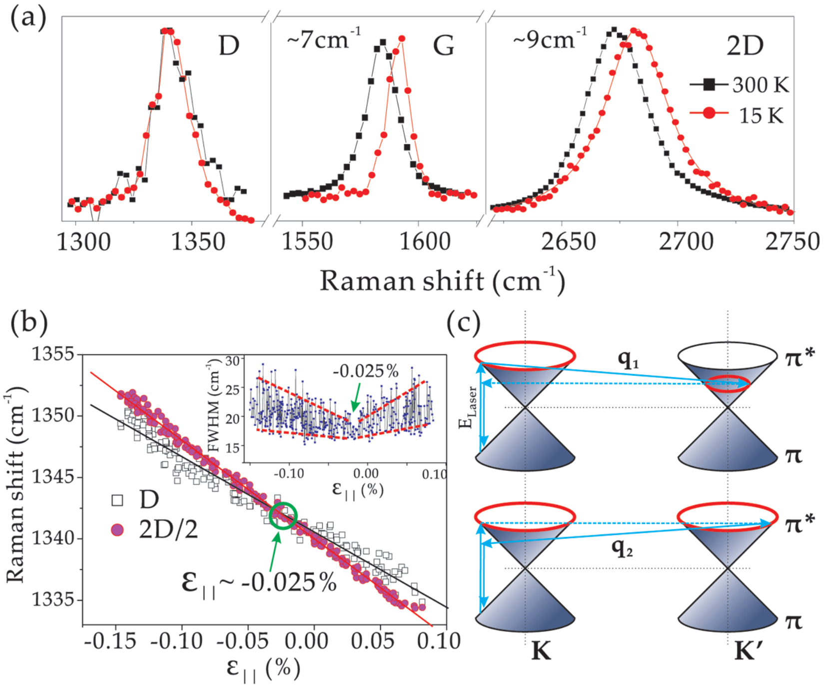

FIGURE 3. (a) D, G, and 2D peaks measured at 300 and 15 K. (b) Half of ω_{2D} plotted together with ω_D as a function of $\varepsilon_{||}$. The two lines show different shifts with applied stain and cross each other at $\sim-0.025\%$. The inset shows the butterfly like pattern of the fwhm of D peak as a function of $\varepsilon_{||}$. (c) Two possible DR mechanisms which involve phonons with slight energy difference.

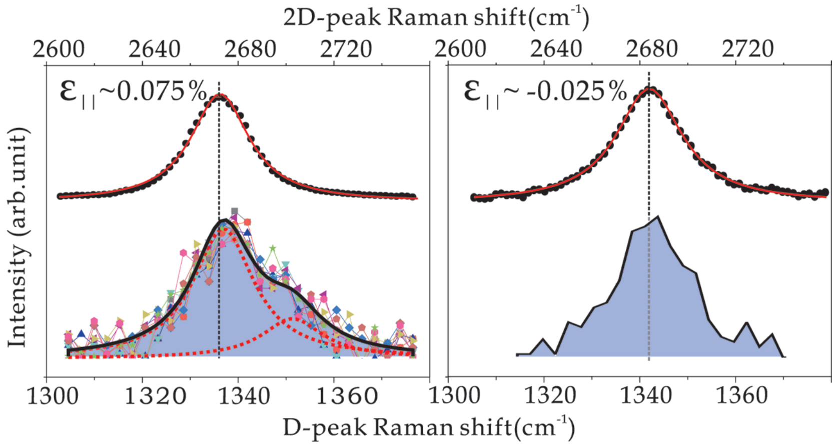

FIGURE 4. Raman spectra of the 2D and the D peaks measured at $\varepsilon_{||}\sim0.075\%$ (left) and at $\varepsilon_{||}\sim-0.025\%$ (right). Note that the horizontal scale of the 2D peak is twice that of the D peak. The measurement of the D peak at $\varepsilon_{||}\sim0.075\%$ is repeated by 10 times to ensure an accurate evaluation of the line shape.

fwhm shows a discrete behavior. Since the D peak is composed by two peaks, they shift differently with applied strain (however, the mechanism is not clear yet) and cross each other at $\varepsilon_{||}\sim-0.025\%$, leading to the butterfly like behavior of the measured D peak fwhm (with minimum values at $\varepsilon_{||}\sim-0.025\%$), see inset of Figure 3b.

We also analyze the line shape of the peaks at $\varepsilon_{||}\sim-0.025\%$ in the right part of Figure 4. The 2D peak does not show significant changes in its fwhm compared to the peak at $\varepsilon_{||}\sim0.075\%$, which is a good indication of the biaxial character of the applied strain.[14] In contrast, the D peak becomes narrower and can be fitted by only one Lorentzian with a fwhm of ~17 cm^{-1}. It is also notable that our data are similar (in both peak position and shape) to a previous report by Ferrari et al.,[26] where a single-Lorentzian for the D peak and $\omega_{2D}/2\sim\omega_D$ were observed. Figures 3 and 4 indicates that the different observations of whether $\omega_{2D}/2$ equals ω_{2D} may due to the different intrinsic strain in the graphene samples.[24−26]

In conclusion, we have presented data on tunable modification of the graphene Raman modes by external biaxial strain. The experiment is realized by utilizing a newly developed piezoelectric actuator-based technique. The key mechanical characteristics of graphene, that is, the

Grüneisen parameters, are studied under biaxial strain that does not change the relative positions of the Dirac cones.[14] The obtained experimental values of Grüneisen parameter are important for validation of theoretical calculations.[19] We observe the peculiar $\omega_{2D}/2 \neq \omega_D$ phenomenon and conclude that the D mode is composed by two peaks as predicted by theories for two-dimensional graphite.[21,22] Another appealing feature of the technique is that it allows to exert strain on demand, that is, the amount of strain on the graphene can be controlled by the applied voltage. A typical voltage step in our experiments of 20 V corresponds to a strain increment of $\sim$0.0028%. In addition to the fundamental insight into the strain-modified Raman modes, the technique reported here features potential for several important applications. For example, mechanical strain has been predicted as an important design tool to engineer graphene's electronic properties[37] and thus affect the ballistic conductance,[38] the basal-plane hydrogenation,[39] and may modify the thermal conductivity of graphene when supported by a substrate.[7,8,40] Combining graphene with the piezoelectric actuator promises new opportunities to study the strain-related behaviors of graphene with unprecedented details.

Acknowledgment. The authors thank L. Zhang, J. D. Plumhof, R. Giraud, J. Maultzsch, M. Mohr, and N. Bonini for fruitful discussions. F.D. acknowledges the support from CAS-MPG program and NSFC China (60625402). H.X.J. is grateful to the Alexander von Humboldt Foundation for fellowship support. Y.F.M. acknowledges the support from the Visiting Scholar Foundation of Key Lab. of Opto-electronic Technology and Systems in Chongqing University.

Note Added after ASAP Publication. Figure 1 was modified in the version of this paper published ASAP August 9, 2010. The correct version published August 12, 2010.

REFERENCES AND NOTES

(1) Geim, A. K.; Novoselov, K. S. *Nat. Phys.* **2007**, *6*, 183–191.
(2) Novoselov, K. S.; Jiang, D.; Schedin, F.; Booth, T. J.; Khotkevich, V. V.; Morozov, S. V.; Geim, A. K. *Proc. Natl. Acad. Sci. U.S.A.* **2005**, *102*, 10451–10453.
(3) Novoselov, K. S.; Geim, A. K.; Morozov, S. V.; Jiang, D.; Zhang, Y.; Dubonos, S. V.; Grigorieva, I. V.; Firsov, A. A. *Science* **2004**, *306*, 666–669.
(4) Novoselov, K. S.; Jiang, Z.; Zhang, Y.; Morozov, S. V.; Stormer, H. L.; Zeitler, U.; Maan, J. C.; Boebinger, G. S.; Kim, P.; Geim, A. K. *Science* **2007**, *315*, 1379.
(5) Zhang, Y.; Tan, Y.-W.; Stormer, H. L.; Kim, P. *Nature* **2005**, *438*, 201.
(6) Du, X.; Skachko, I.; Barker, A.; Andrei, E. Y. *Nat. Nanotechnol.* **2008**, *3*, 491.
(7) Balandin, A. A.; Ghosh, S.; Bao, W.; Calizo, I.; Teweldebrhan, D.; Miao, F.; Lau, C. N. *Nano Lett.* **2008**, *8*, 902–907.
(8) Seol, J. H.; Jo, I.; Moore, A. L.; Lindsay, L.; Aitken, Z. H.; Pettes, M. T.; Li, X.; Yao, Z.; Huang, R.; Broido, D.; Mingo, N.; Ruoff, R. S.; Shi, L. *Science* **2010**, *328*, 213–216.
(9) Lee, C.; Wei, X.; Kysar, J. W.; Hone, J. *Science* **2008**, *321*, 385.
(10) Zhou, S. Y.; Gweon, G. H.; Fedorov, A. V.; First, P. N.; de Heer, W. A.; Lee, D. H.; Guinea, F.; Castro Neto, A. H.; Lanzara, A. *Nat. Phys.* **2007**, *6*, 770.
(11) Teague, M. L.; Lai, A. P.; Velasco, J.; Hughes, C. R.; Beyer, A. D.; Bockrath, M. W.; Lau, C. N.; Yeh, N. C. *Nano Lett.* **2009**, *9*, 2542–2546.
(12) Guinea, F.; Katsnelson, M. I.; Geim, A. K. *Nat. Phys.* **2009**, *6*, 30–33.
(13) Ni, Z. H.; Yu, T.; Lu, Y. H.; Wang, Y. Y.; Feng, Y. P.; Shen, Z. X. *ACS Nano* **2008**, *2*, 2301.
(14) Mohiuddin, T. M. G.; Lombardo, A.; Nair, R. R.; Bonetti, A.; Savini, G.; Jalil, R.; Bonini, N.; Basko, D. M.; Galiotis, C.; Marzari, N.; Novoselov, K. S.; Geim, A. K.; Ferrari, A. C. *Phys. Rev. B* **2009**, *79*, 205433.
(15) Huang, M.; Yan, H.; Chen, C.; Song, D.; Heinz, T. F.; Hone, J. *Proc. Natl. Acad. Sci. U.S.A.* **2009**, *106*, 7304.
(16) Yu, T.; Ni, Z.; Du, C.; You, Y.; Wang, Y.; Shen, Z. *J. Phys. Chem. C* **2008**, *112*, 12602.
(17) Tsoukleri, G.; Parthenios, J.; Papagelis, K.; Jalil, R.; Ferrari, A. C.; Geim, A. K.; Novoselov, K. S.; Galiotis, C. *Small* **2009**, *5*, 2397–2402.
(18) Nika, D. L.; Pokatilov, E. P.; Askerov, A. S.; Balandin, A. A. *Phys. Rev. B* **2009**, *79*, 155413.
(19) Nika, D. L.; Ghosh, S.; Pokatilov, E. P.; Balandin, A. A. *Appl. Phys. Lett.* **2009**, *94*, 203103.
(20) Metzger, C.; Rémi, S.; Liu, M.; Kusminskiy, S. V.; Castro Neto, A. H.; Swan, A. K.; Goldberg, B. B. *Nano Lett.* **2010**, *10*, 6–10.
(21) Cançado, L. G.; Pimenta, M. A.; Saito, R.; Jorio, A.; Ladeira, L. O.; Grueneis, A.; Souza-Filho, A. G.; Dresselhaus, G.; Dresselhaus, M. S. *Phys. Rev. B* **2002**, *66*, No. 035415.
(22) Maultzsch, J.; Reich, S.; Thomsen, C. *Phys. Rev. B* **2004**, *70*, 155403.
(23) Tan, P.; Hu, C.; Dong, J.; Shen, W.; Zhang, B. *Phys. Rev. B* **2001**, *64*, 214301.
(24) Ni, Z. H.; Wang, H. M.; Ma, Y.; Kasim, J.; Wu, Y. H.; Shen, Z. X. *ACS Nano* **2008**, *2*, 1033–1039.
(25) Dong, X.; Shi, Y.; Zhao, Y.; Chen, D.; Ye, J.; Yao, Y.; Gao, F.; Ni, Z.; Yu, T.; Shen, Z.; Huang, Y.; Chen, P.; Li, L.-J. *Phys. Rev. Lett.* **2009**, *102*, 135501.
(26) Ferrari, A. C.; Meyer, J. C.; Scardaci, V.; Casiraghi, C.; Lazzeri, M.; Mauri, F.; Piscanec, S.; Jiang, D.; Novoselov, K. S.; Roth, S.; Geim, A. K. *Phys. Rev. Lett.* **2006**, *97*, 187401.
(27) Thomsen, C.; Reich, S. *Phys. Rev. Lett.* **2000**, *85*, 5214.
(28) Saito, R.; Jorio, A.; Souza Filho, A. G.; Dresselhaus, G.; Dresselhaus, M. S.; Pimenta, M. A. *Phys. Rev. Lett.* **2001**, *88*, No. 027401.
(29) Proctor, J. E.; Gregoryanz, E.; Novoselov, K. S.; Lotya, M.; Coleman, J. N.; Halsall, M. P. *Phys. Rev. B* **2009**, *80*, No. 073408.
(30) Hanfland, M.; Beister, H.; Syassen, K. *Phys. Rev. B* **1989**, *39*, 12598.
(31) Sandler, J.; Shaffer, M. S. P.; Windle, A. H.; Halsall, M. P.; Montes-Morán, M. A.; Cooper, C. A.; Young, R. J. *Phys. Rev. B* **2003**, *67*, No. 035417.
(32) Ding, F.; Singh, R.; Plumhof, J. D.; Zander, T.; Křápek, V.; Chen, Y. H.; Benyoucef, M.; Zwiller, V.; Dörr, K.; Bester, G.; Rastelli, A.; Schmidt, O. G. *Phys. Rev. Lett.* **2010**, *104*, 067405.
(33) Zander, T.; Herklotz, A.; Kiravittaya, S.; Benyoucef, M.; Ding, F.; Atkinson, P.; Kumar, S.; Plumhof, J. D.; Dörr, K.; Rastelli, A.; Schmidt, O. G. *Opt. Express* **2009**, *17*, 22452.
(34) Calizo, I.; Miao, F.; Bao, W.; Lau, C. N.; Balandin, A. A. *Appl. Phys. Lett.* **2007**, *91*, No. 071913.
(35) Allen, M. J.; Fowler, J. D.; Tung, V. C.; Yang, Y.; Weiller, B. H.; Kaner, R. B. *Appl. Phys. Lett.* **2008**, *93*, 193119.
(36) Wang, Y.; Alsmeyer, D. C.; McCreery, R. L. *Chem. Mater.* **1990**, *2*, 557.
(37) Choi, S. M.; Jhi, S. H.; Son, Y. W. *Phys. Rev. B* **2010**, *81*, No. 081407.
(38) Hossain, M. Z. *Appl. Phys. Lett.* **2010**, *96*, 143118.
(39) Xue, K.; Xu, Z. *Appl. Phys. Lett.* **2010**, *96*, No. 063103.
(40) Xu, Z.; Buehler, M. J. *Nanotechnology* **2009**, *20*, 185701.